

NUMERICAL PREDICTIONS OF THE FLOW AROUND A SMALL DUCTED WIND TURBINE EQUIPPED WITH PASSIVE FLOW CONTROL DEVICES

Costin Ioan COȘOIU, Andrei Mugur GEORGESCU, Mircea DEGERATU, Alexandru Cezar VLĂDUȚ,
Elena-Alexandra CHIULAN

Technical University of Civil Engineering Bucharest

Corresponding author: Costin Ioan COȘOIU, E-mail: costin@hidraulica.utcb.ro

Abstract. On sites where the wind is blowing at low velocities or in urban environment, classic aeolian turbines are working inefficiently. The performances of wind turbines can possibly be augmented using casings that work as concentrating devices for the scattered low speed wind. An innovative casing design is proposed to shroud an axial wind turbine rotor. In order to increase the flow through the turbine rotor and subsequently the energy extracted from the main flow, the casing is equipped with air injection slots that are working as passive flow control devices. The global performances of the ducted wind turbine are evaluated by means of numerical simulations. These are compared with the characteristics of the bare turbine rotor and also with another ducted turbine, with a similar rotor but using a previously proposed casing.

Key words: passive flow control, profiled case, wind energy, wind turbine, flow separation, CFD.

1. INTRODUCTION

The aeolian energy was converted and used since ancient times [1], but the lack of knowledge on the aerodynamic aspects involved in the design, development and production cycles, placed it in an incipient stage until the second half of the 20th century [2]. The oil shock from the 8th decade of the last century imposed a new perspective on the need to discover or to improve existing energy production technologies [3]. The wind energy, in the context of accelerated reduction of more conventional energy resources, coupled with increasing demand for energy, arises as a viable solution to compensate such shortfall [4].

Starting from early 1980's the technology developed, and the production capacity grew. In 1980, the global installed capacity was equal to 10 MW [5]. In 1997 it grew to 7.6 GW [5] and at the end of 2016 the world wind generation capacity reached 539 GW, around 8% of the total global power generation capacity [6, 7].

Currently, the technology for production and implementation of aeolian solutions is a mature one, yet far from reaching its limits [8]. Although, the industry had an exponential growth, as illustrated in Fig. 1a, some issues appeared in the wind energy production domain, in the context of an accelerated dynamics in the first decades of the 21st Century. These issues can be summarized as follows:

1. Availability of sites with good wind potential. Modern wind turbines produce energy efficiently from mean wind speeds of 7 m/s or higher [9]. In areas where the wind frequently blows at lower speeds, the energy from wind turbines cannot be collected using classical means. In Romania, for example, the frequency distribution of the wind speed occurrence has a maximum in the lower velocity region, approximately 5 m/s, for more than 70% of this country's territory.

2. The random character of exploited energy source and low capacity factor of present wind turbines. According to the European Wind Energy Association, in 2016, the total installed power of wind turbines in Romania was 3129 MW [10]. Although, Dobrogea is the best 2nd site in Europe for wind energy harvesting operations, due to random operation nature of the wind turbines, determined by weather conditions and complicated maintenance works necessary for big units, the total produced energy was equal to only 1/4 of the maximum amount of energy that could be produced. The wind energy production in Romania in 2016 is presented in Fig. 1b, emphasizing the average production and total installed capacity [11].

3. New demands from society and development of new technologies which implies the emergence of a new market targeted to household consumers, small communities in developing regions with low or no access to existing power grid. New developments in battery technologies, along with the development of solar panels, are opening a new niche in the energy production market: hybrid wind-solar small energy production systems connected to a battery, able to supply energy for Nearly Zero-Energy Buildings (nZEB) or passive houses, irrespective of weather conditions, suggests a well-balanced energy production, with almost equal mean values for harvested wind and solar energy.

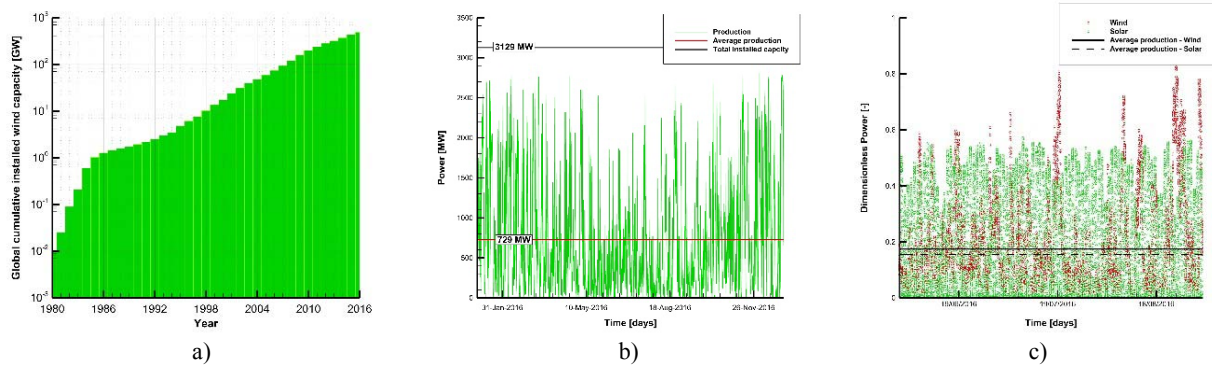


Fig. 1 – a) Global cumulative installed wind capacity 1980-2016 [6, 7]; b) wind energy production in Romania, in 2016 [11]; c) dimensionless wind and solar production in Romania, summer period, in 2016 [11].

When analyzing the dimensionless energy production, on a three-month period during the summer (from 1st of June to 31st of August) of 2016, in Romania [11], one may observe that the capacity factor for wind and solar have nearly similar values (Fig. 1c). However, when the analysis is performed for a 1-year period, for the same years, the average energy production from wind is higher than the mean energy from solar. This is due to the fact that in Romania, the solar installed capacity is still at a lower level when compared to wind and also due to the low efficiency of the present solar panels when they are used in winter time.

One possible solution in order to use wind turbines in sites with low wind speed, is to locally increase the wind speed, in the rotor area. This can be achieved by augmenting the air flow using a wind concentrator casing mounted around the turbine. So, the power output of the turbine is substantially increased, since it varies with the third power of the wind speed. The usage of ducted wind turbines ensures the possibility of concentrating the wind energy, even at low wind conditions, and thus obtaining a higher capacity factor. Last, but not least, ducted wind turbines have a lower noise level [12] when compared to free horizontal axis wind turbines [13].

2. SMALL DUCTED WIND TURBINES EQUIPPED WITH PASSIVE FLOW CONTROL DEVICES CONCEPT

At the Hydraulic and Environmental Protection Department of the Technical University of Civil Engineering in Bucharest, a new energy production technology using small ducted wind turbines equipped with passive flow control devices is developed. A casing was tested, and promising results were obtained regarding its performances [14]. It is able to ensure a higher volumetric flow rate in the rotor active section so that for a given wind turbine, when compared to the bare unit, an increase with a factor up to 2.75 can be obtained. The performance of the casing is based on four aerodynamic effects given by four separate concepts that were previously studied in other researches for wind turbine power output augmentation and were combined in an integral approach for an increased efficiency.

The first concept implies that the casing has the interior profile of a convergent-divergent nozzle, to obtain a concentration effect that leads to air acceleration in the throat of the nozzle [15,16]. Bet and Grassman [17] considered a ring-wing type wind concentrator. This second concept was also taken into account when the casing profile was designed. It is based on an airfoil with high lift and high lift to drag ratio. The third concept proposed a casing with injection slots for boundary layer separation control [18, 19].

These slots are connecting the exterior part of the casing where the static pressure is higher with the interior part where the static pressure is lower. The last concept adopted in the casing design process assumes a high divergent angle of the nozzle. This ensures flow separation at the trailing edge of the casing, creating a pair of vortices that are traveling downstream, following a pattern similar to von Karman's vortex street. The static pressure downstream the casing is dropping, leading to a higher flow rate through the wind turbine rotor section.

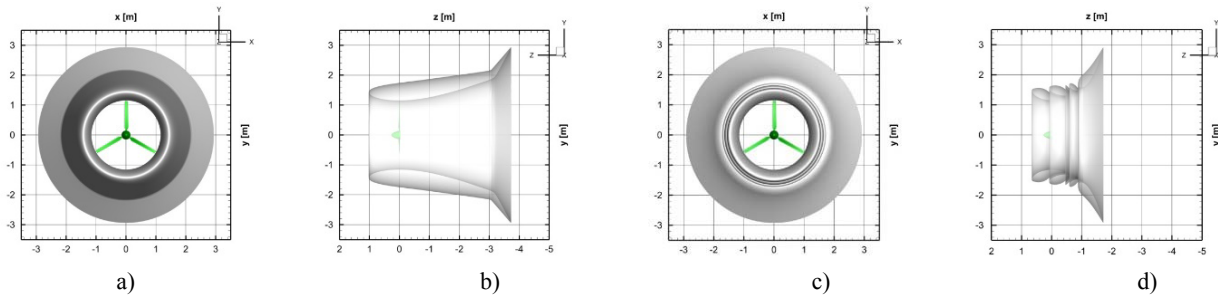


Fig. 2 – The SICE-1kW wind turbine shrouded using the v-1 casing: a) front view; b) lateral view; The SICE-1kW wind turbine shrouded using the v11 casing: c) front view; d) lateral view.

The proposed casing designed to satisfy all the above-mentioned conditions is presented in (Fig. 2c and Fig. 2d). This casing is named v11 and it was developed starting from an earlier design proposed by Coşoiu et al. [20], named v-1 (Fig. 2a and Fig. 2b). The v-1 casing has a ring wing shape, generated by revolving over 360° a NACA4412 airfoil with an angle of attack of 10° around a symmetry axis. At the exit area, a large opening angle was obtained by adding a 20° angle of attack to the airfoil starting from 80% of the chord length. The casing profile has a convergent-divergent interior shape due to the airfoil geometry used to design the casing.

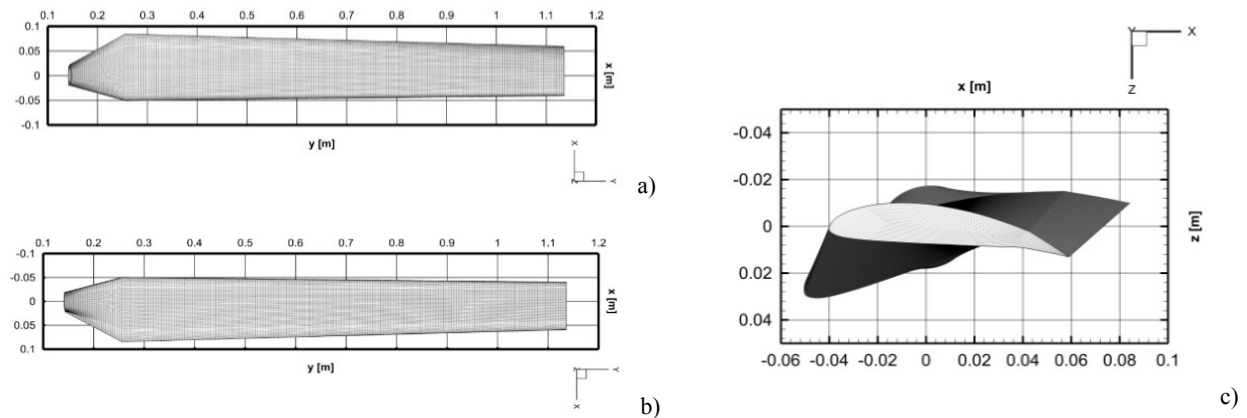


Fig. 3 – The SICE-1 kW rotor blade: a) upper part; b) lower part; c) view from the blade tip.

The v11 casing is derived from the v-1 shape. It has the same exit diameter and the same throat diameter, but the axial length (L) is reduced by half. For the v11 version, in order to reattach the boundary layer at the interior of the casing, four injecting slots are provided. In the present numerical study, the stiffening ribs necessary to keep together the v11 casing parts were not modeled.

The investigated wind turbine used in conjunction with the proposed casing is named SICE-1kW and is a small domestic horizontal axis unit, with a rated power of 1kW. Its rotor has a diameter (D) of 2.272 m and the number of blades is equal to 3. The SICE750 airfoil [21] was used to generate the blades. The blade has a linear taper and twist. At the blade tip, the chord (c) is equal to 0.09 m. The maximum chord length is found in the section placed at $r=0.256$ m from the rotor axis of rotation and is equal to 0.14 m. The maximum blade twist is equal to 18° . Between the cylindrical shaft that attaches the blades to the hub and the $r=0.256$ m section, the blade root is characterized by a smooth geometrical transition. The SICE-1kW turbine blade is presented in Figs. 3 a,b,c.

3. NUMERICAL MODEL AND COMPUTATIONAL CONDITIONS

3.1. General hypothesis

The numerical study on the small ducted wind turbine was conducted using a similar method previously used by Coșoiu et al. [20] on the NREL Phase VI experimental test case [23]. In previous works of Sørensen et al. [24] and Mahu and Popescu [25], a similar approach was used with good results.

Thus, the flow was assumed to be circumferentially symmetrical, rotationally periodic and aligned with the axis of rotation. The Moving Reference Frame (MRF) model was used to simulate the wind turbine rotor rotation. In the MRF model, the equations of motion are modified to incorporate the additional acceleration terms which occur due to the transformation from the stationary to the moving reference frame [22]. Thus, the flow around the blades can be modelled by solving these equations in a steady-state manner.

The fluid domain viewed in a moving reference frame was considered to rotate with an angular velocity ω specific to different tip speed ratios λ . The tip speed ratio was defined as:

$$\lambda = \omega D / 2u_{\infty}, \quad (1)$$

where u_{∞} is the velocity at the inlet boundary.

Corresponding to different rotational speeds of the turbine rotor, the Reynolds number at the blade tip, computed using:

$$\text{Re} = \rho c \sqrt{u_{\infty}^2 + (0.5\omega D)^2} / \mu \quad (2)$$

varied accordingly. In equation (2), ρ and μ are the air density and air dynamic viscosity, respectively.

3.2. The turbulence model

For all the performed simulations, in order to minimize the allocated computational resources and optimize the time dedicated for the simulations, the viscous pressure-based k - ω SST turbulence model implemented in the ANSYS FLUENT commercial software was used.

The model uses RANS decomposition for the momentum and continuity equations as follows:

$$\frac{\partial \bar{u}_i}{\partial x_i} = 0, \quad (3)$$

$$\bar{u}_j \frac{\partial \bar{u}_i}{\partial x_j} = -\frac{1}{\rho} \frac{\partial p}{\partial x_i} + \frac{\partial}{\partial x_j} \left[\nu \left(\frac{\partial \bar{u}_i}{\partial x_j} + \frac{\partial \bar{u}_j}{\partial x_i} \right) - \overline{u'_i u'_j} \right]. \quad (4)$$

In equations (3) and (4), ρ , \bar{p} , \bar{u}_i , \bar{u}'_i and ν denote the density, the mean static pressure, the mean static velocity, the mean turbulent velocity fluctuations and the kinematic viscosity, respectively.

A Boussinesq hypothesis is considered to model the Reynolds stresses in order to solve the closure problem. Accordingly, the turbulent viscosity is computed by introducing two additional transport equations for the turbulence kinetic energy (k) and its specific dissipation rate (ω):

$$\frac{\partial}{\partial x_i} (k \bar{u}_i) = \frac{1}{\rho} \left[\frac{\partial}{\partial x_j} \left(\Gamma_k \frac{\partial k}{\partial x_j} \right) + \tilde{G}_k - Y_k \right], \quad (5)$$

$$\frac{\partial}{\partial x_i} (\omega \bar{u}_i) = \frac{1}{\rho} \left[\frac{\partial}{\partial x_j} \left(\Gamma_{\omega} \frac{\partial \omega}{\partial x_j} \right) + G_{\omega} - Y_{\omega} + D_{\omega} \right]. \quad (6)$$

In equations (5) and (6), Γ_k , \tilde{G}_k , Y_k , Γ_{ω} , G_{ω} , Y_{ω} and D_{ω} denote the effective diffusivity of k , the generation of turbulent kinetic energy due to the mean velocity gradients, the dissipation of k due to

turbulence, the effective diffusivity of ω , the generation of ω , the dissipation of ω due to turbulence and the cross-diffusion term, respectively.

For the simulations, second-order discretization schemes were used for pressure, the momentum equation and the transport equations for the specific turbulence model parameters. All the simulations were performed using a double precision pressure-based coupled solver.

3.3. The grid and computational conditions. Small ducted wind turbine equipped with passive flow control devices – v11 casing

Considering the circumferential symmetrical flow hypothesis, the fluid domain was generated in the shape of a sliced cylinder with the height aligned with the turbine axis of rotation (Fig. 4a). The radius of the cross-section of the fluid domain is equal to 5.72 rotor diameters. The MRF formulation implies that the fluid domain is divided in two zones: a stationary one and another that is rotating with the blade. In Fig. 4b, the rotating zone can be observed. On the lateral cylindrical surface of the fluid domain, a slip condition was set. The rectangular surfaces placed in the domain symmetry plane were set up as periodical boundaries. The exit section diameter of the casing is equal to $2.57D$. The inlet section is placed at 2.2 turbine rotors diameters, upstream the turbine rotor, while the exit section is placed downstream of it, at 11 rotor diameters.

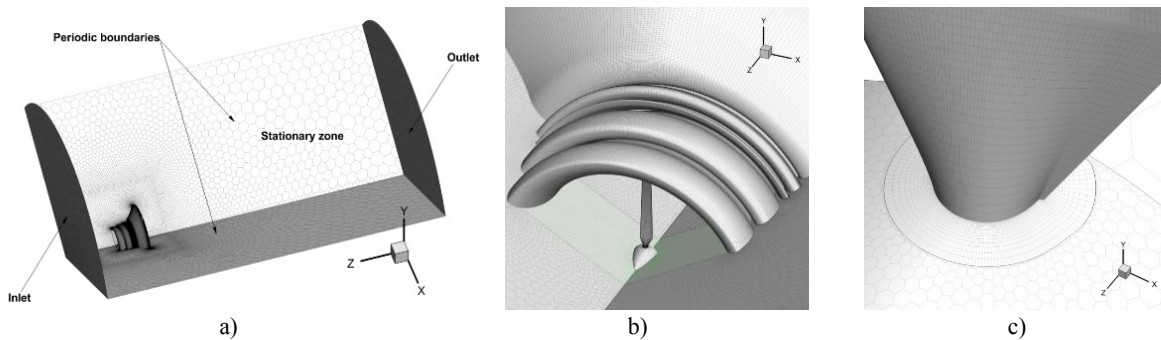


Fig. 4 – The grid and computational conditions: a) a general view of the mesh and boundary conditions; b) mesh detail near the ducted turbine; c) grid detail at the blade root.

At the inlet boundary, the axial velocity (u_∞) was set to a constant value of 6.5 m/s. The radial velocity was set to 0. At the inlet boundary, the turbulence intensity (I_∞) was set to a constant value of 0.02, corresponding to a low turbulent wind and the turbulence length scale (l_∞) was set to be equal to the turbine rotor diameter (D). At the outlet boundary, the static pressure (p_e) was set to 0-gauge scale. The blades and the hub of the rotor were set up as moving walls, with a 0 rad/s angular-velocity relative to adjacent cell zone.

The grid has a mixed structure. It was composed of a total number of 1 757 296 hexahedral and polyhedral cells. The blade surface was meshed using 33 100 quad cells. The minimum cell characteristic length was equal to $0.001c$, near the leading edge and the trailing edge of the blade. In order to ensure a proper y^+ distribution, necessary for the turbulent model to correctly compute the flow, in the boundary layer zone, near the blade, eighteen layers of prismatic cells, normal to the blade surface, were constructed. They were distributed in a geometrical progression with a height increase ratio between two successive layers of 1.2. The first layer height was equal to $0.001c$. In Fig. 4c, a detail of the mesh at the blade root is presented.

On the solid surfaces of the casing, quad cells were mainly used. On the no slip boundary of the casing which is also part of the rotating fluid domain, the discretization was made using polygonal cells. On the casing surfaces, the cells dimensions varied between $0.1c$ and $0.55c$ (Fig. 4b). In the remnant of the fluid domain, polyhedral cells were used to minimize the computational effort and also to improve the quality of the final numerical solution. In the rotating fluid zone, the maximum cell size was equal to $1.11c$. In the stationary fluid domain, their maximum characteristic length was equal to $11c$.

4. RESULTS AND DISCUSSION

The global performances of the ducted SICE-1kW horizontal axis wind turbine using the v11 casing were quantified (Moment coefficient C_M and Power coefficient C_P) and compared to the corresponding values that characterize the bare turbine rotor. Also, a comparison was made between the global performances of the shrouded turbine using the v11 casing and the global performances of the shrouded turbine using the v-1 casing [20].

The moment coefficient C_M is given by $C_M = M_Z / 0.25\rho A D u_\infty^2$, where M_Z is the torque computed with respect to the rotation axis of the turbine and A is the turbine rotor cross-section area. The power coefficient C_P is given by $C_P = P / 0.5\rho A u_\infty^3$, where P is the power at the turbine shaft.

In Fig. 5a the power coefficient C_P variations for different tip speed ratios λ is presented for the bare wind turbine, as well as for the ducted turbine using the v-1 casing and v11 casing, respectively. The optimal operating point of the v11 ducted turbine was obtained for a tip speed ratio $\lambda=6.67$. The corresponding computed power coefficient is equal to 1.32. When compared to the bare wind turbine, the predicted, maximum power coefficient, increases with a factor up to 2.49. The v11 ducted wind turbine has a lower efficiency at lower tip speed ratios, while, at higher tip speed ratios, the power coefficient is higher than the corresponding values computed for the other cases. The v-1 casing is providing a better efficiency when it is coupled with the wind turbine than the bare turbine itself, but, when compared to the v11 ducted turbine, a decrease of 6.45% in efficiency is detected. As the efficiency increases, when switching from the bare turbine to the v-1 ducted turbine and then to the v11 ducted turbine, an increase of the tip speed ratio is also observed. This implies higher angular-velocities that are determined by higher flow rates through the active section of the rotor.

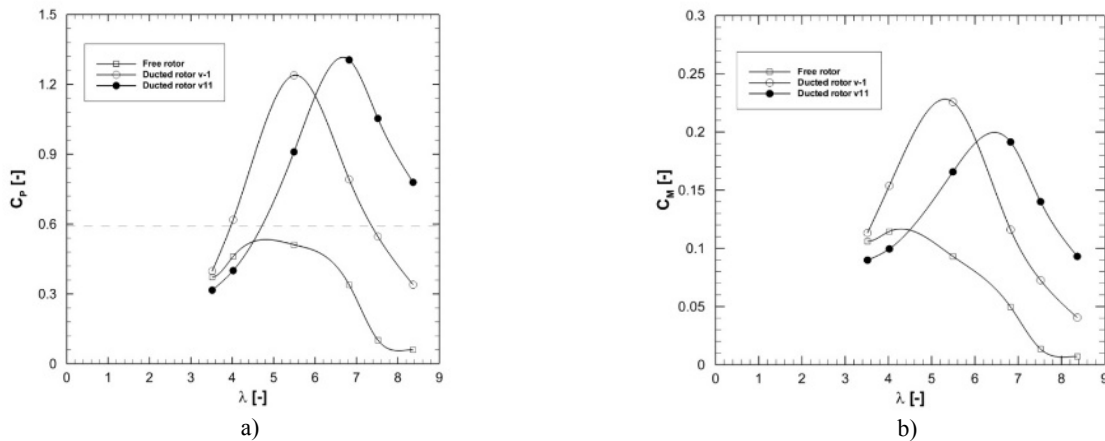


Fig. 5 – a) Power coefficient C_P variation as a function of the tip speed ratio λ ;
b) moment coefficient C_M variation as a function of the tip speed ratio λ .

The moment coefficient C_M variations for different tip speed ratio λ for the bare wind turbine, and for the ducted wind turbine, using v-1 and v11 casings, respectively, are presented in Fig. 5b. The same trends as in the power coefficients case are observed. The maximum moment coefficient was found to correspond to the optimal operating point, where the power coefficient has also a maximum value. However, when comparing the v-1 and v11 cases, one can observe that for the optimal operating point, in the case of v-1 casing, a larger torque at the turbine shaft is predicted. A smaller moment at the v11 turbine shaft implies smaller loads on the mechanical components of the unit. A higher angular velocity implies a less complex gearbox or no gearbox at all between the turbine rotor and the generator.

The higher energy output of the v11 wind turbine is obtained due to an increased air flow through the rotor. For the v-1 version, the increase in volumetric flow rate is explained solely by the concentrating effect of the casing. In the case of the v11 casing, the existence of the injecting slots brings a supplement of air flow into the casing throat due to flow stabilization in the boundary layer zone, near the interior surface of the duct.

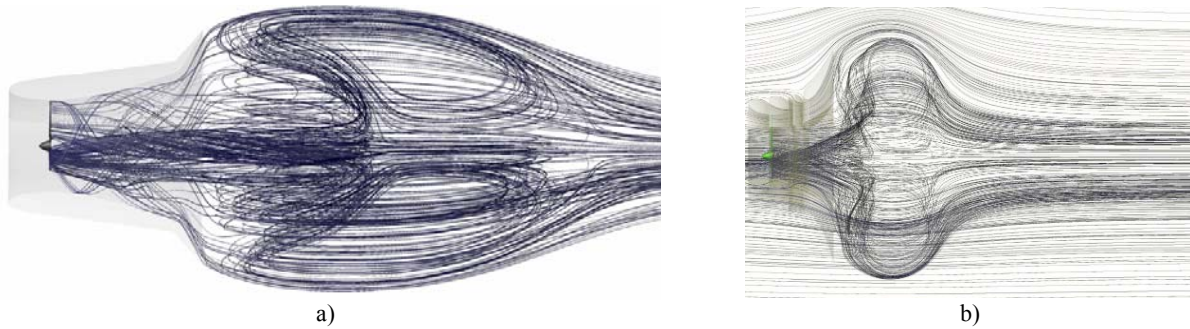


Fig. 6 – a) Streamlines around the v-1 ducted wind turbine; b) streamlines around the v11 ducted wind turbine.

In Fig. 6a, streamlines around the v-1 ducted wind turbine are presented. The predicted characteristic length of the ring vortex downstream the v-1 casing is equal to $4.15L$ (i.e. 2.13 v-1 case lengths). When inspecting the streamlines around the v11 ducted wind turbine presented in Fig. 6b, one may observe that the ring vortex downstream the turbine, generated due to flow separation at the trailing edge of the casing, is pushed downstream by the air jets injected through the flow control devices. The same behavior was previously predicted by Coşoiu et al. [14] for the same casing placed in a uniform velocity field, without the turbine rotor installed. This favorable effect is preserved also when the turbine is shrouded by the casing. The predicted characteristic length of the ring vortex downstream the v11 casing is equal to $1.29L$, suggesting a higher efficiency of the v11 casing when compared to the v-1 version. Near the solid boundary of the v11 casing, the flow remains attached, less energy from the main flow being consumed in order to keep alive the downstream ring vortex.

5. CONCLUSIONS

Currently, wind turbine technology is a mature one, yet far from reaching its limits. In areas with a higher probability of low wind speed, installing wind turbines it is not economically feasible.

Sustaining development for a dynamic society in a smart city, demands clean energy to be gathered near the household consumers. In order to cope with these problems, a new concept for a small ducted wind turbine equipped with passive flow control devices is proposed.

Multiple steady numerical simulations were performed in order to predict the global performances of a ducted horizontal axis wind turbine using a casing equipped with passive flow control devices. A moving reference frame was considered in order to simulate the rotational effects of the rotor.

The casing has a reduced axial dimension in order to minimize the weight of the unit. The casing shape was designed by superposing several aerodynamic effects with favorable consequences on the turbine performances. The most important effect is obtained by the air injecting slots that are energizing the boundary layer, delaying its separation.

The numerical simulations predicted an increase in efficiency with a factor of up to 2.49 for the shrouded turbine with respect to the bare one. This design offered better performances than a previous proposed casing. An increase of the power coefficient with a factor of up to 1.06 was determined for the newly proposed version with respect to the old one.

For the optimal operating point, the ducted turbine equipped with passive flow control devices works at higher angular-velocities than the bare one and other previous proposed version of ducted wind turbines, due to a higher flow rate through the turbine rotor.

ACKNOWLEDGEMENTS

The authors acknowledge the support from the Executive Unit for Financing of the Higher Education, Research, Development and Innovation grants (UEFISCDI PN-II PD-193 105/2010 and PN-III-P2-2.1-PED-2016-0631). All numerical simulations have been performed at the Hydraulics and Environmental Protection Department from the Technical University of Civil Engineering of Bucharest.

REFERENCES

1. P. D. FLEMING, S. D. PROBERT, *The evolution of wind-turbines: An historical review*, Applied Energy, **18**, pp. 163-177, 1984.
2. R. L. HILLS, *Power from wind: a history of windmill technology*, Cambridge University Press, Cambridge, 1994.
3. D. CARMOY, *The USA faces the energy challenge*, Energy Policy, **6**, 1, pp. 36-52, 1978.
4. J. K. KALDELLIS, D. ZAFIRAKIS, *The wind energy (r)evolution: A short review of a long history*, Renewable Energy, **36**, pp. 1887-1901, 2011.
5. GLOBAL WIND ENERGY COUNCIL, *Global Wind Report – Annual Market Update 2015* (online), available at: <http://www.gwec.net/publications/global-wind-report-2/global-wind-report-2015-annual-market-update/>, 2016, Accessed on May 2018.
6. WORLD ENERGY COUNCIL, *World Energy Resources*, ISBN 978-0-946121-62-5, 2016.
7. GLOBAL WIND ENERGY COUNCIL, *Global Wind Statistics 2017* (online), available at: http://gwec.net/wp-content/uploads/vip/GWEC_PRstats2017_EN-003_FINAL.pdf, Accessed on May 2018.
8. J. F. MANWELL, J. G. MCGOWAN, A. L. ROGERS, *Wind Energy Explained: theory, design and application*, 2nd Edition, John Wiley and Sons Ltd., ISBN 978-0-470-01500-1, 2009.
9. G. M. JOSELIN HERBERT, S. INIYANB, E. SREEVALSANC, S. RAJAPANDIAN, *A review of wind energy technologies*, Renewable and Sustainable Energy Reviews, **11**, pp. 1117-1145, 2007.
10. EUROPEAN WIND ENERGY ASSOCIATION, *Wind in power. 2015 European statistics* (online), available at: <http://www.ewea.org/fileadmin/files/library/publications/statistics/EWEA-Annual-Statistics-2015.pdf>, 2016, Accessed on March 2018.
11. TRANSELECTRICA, *Grafic producția, consumul și soldul SEN* (in Romanian) (online), available at: http://www.transelectrica.ro/widget/web/tel/sen-grafic/-/SENGrafic_WAR_SENGraficportlet, 2017, Accessed on November 2017.
12. W. X. WANG, T. MATSUBARA, J. HU, S. ODAHARA, T. NAGAI, T. KARASUTANI, Y. OHYA, *Experimental investigation into the influence of the flanged diffuser on the dynamic behavior of CFRP blade of a shrouded wind turbine*, Renewable Energy, **78**, pp. 386-397, 2015.
13. H. DUMITRESCU, V. CARDOȘ, A. DUMITRACHE, F. FRUNZULICĂ, *Low-frequency noise prediction of vertical axis wind turbines*, Proceedings of the Romanian Academy – Series A, **11**, 1, pp. 47-54, 2010.
14. C. I. COȘOIU, A. M. GEORGESCU, M. DEGERATU, D. HLEVCA, *Numerical predictions of the flow around a profiled casing equipped with passive flow control devices*, Journal of Wind Engineering and Industrial Aerodynamics, **114**, pp. 48-61, 2013.
15. G. M. LILLEY, W. J. RAINBIRD, *A preliminary report on the design and performance of ducted windmills*, Report no. 102, College of Aeronautics, Cranfield, UK, 1956.
16. F. WANG, L. BAI, J. FLETCHER, J. WHITEFORD, D. CULLEN, *The methodology for aerodynamic study on a small domestic wind turbine with scoop*, Journal of Wind Engineering and Industrial Aerodynamics, **96**, pp. 1-24, 2008.
17. F. BET, H. GRASSMANN, *Upgrading conventional wind turbines*, Renewable Energy, **28**, pp. 71-78, 2003.
18. B. L. GILBERT, K. M. FOREMAN, *Experiments with a diffuser-augmented model wind turbine*, Trans. ASME, Journal of Energy Resources Technology, **105**, pp. 46-53 1983.
19. O. IGRA, *Research and development for shrouded wind turbines*, Energy Conversion and Management, **2113**, p. 48, 1981.
20. C. I. COȘOIU, R. M. DAMIAN, M. DEGERATU, A. M. GEORGESCU, D. HLEVCA, *Numerical study on the efficiency between the ducted and the free stream rotor of a horizontal axis wind turbine*, Proceedings of the EWEA 2011 Conference, Brussels, Belgium, 14-17 March 2011.
21. M. PREDESCU, M. DEGERATU, C. NAE, A. BEJENARIU, O. MITROI, *Measuring power curves of wind turbine rotor in wind tunnel*, Scientific Bulletin of the Politehnica University of Timisoara, Transactions on Mechanics, **52**, pp. 45-53, 2008.
22. ANSYS Inc., *Fluent 13.0 Users Guide*, 2010.
23. M. M. HAND et al., *Unsteady aerodynamics experiment Phase VI: Wind tunnel test configurations and available data campaigns*, NREL/TP-500-29955, NREL, Golden, CO, 2001.
24. N. N. SØRENSEN, J. JOHANSEN, S. CONWAY, *Navier-Stokes predictions of the NREL Phase VI rotor in the NASA Ames 80 ft × 120 ft wind tunnel*, Wind Energy, **5**, pp. 151-169, 2002.
25. R. MAHU, F. POPESCU, *NREL Phase VI modelling and simulation using ANSYS FLUENT 12.1*, Scientific Journal of the Technical University of Civil Engineering. Mathematical Modeling in Civil Engineering, **1-2**, pp. 185-194, 2011.

Received August 27, 2018